

Nonlinear Mechanical Behavior of Scarcely Crosslinked Poly(dimethyl siloxane) Gel: Effect of Strand Length Polydispersity

By Hideaki TAKAHASHI,^{1,2} Yoshitaka ISHIMURO,¹ and Hiroshi WATANABE^{2,*}

Nonlinear mechanical behavior was examined for a scarcely crosslinked poly(dimethyl siloxane) gel (referred to as Gel-1/1) under constant-rate elongation and large step shear strains. The average molecular weight of the gel strands evaluated from the equilibrium modulus in the linear viscoelastic regime was $M_c = 190 \times 10^3$, and the strands had a significantly broad molecular weight distribution, $M_w/M_n \cong 600$ as estimated by fitting the linear viscoelastic moduli with a Rouse network model. In the elongational test at constant elongational rates $\dot{\epsilon}$ ($= \dot{\lambda}/\lambda$; λ = elongational ratio), the Gel-1/1 sample exhibited $\dot{\epsilon}$ -insensitive strain hardening followed by rupture at $\lambda_{\max} = 4.5$. This λ_{\max} was significantly smaller than the λ_{\max}° nominally expected for a gel composed of monodisperse strands having $M_c = 190 \times 10^3$; $\lambda_{\max}^\circ = 53$ and $\lambda_{\max}/\lambda_{\max}^\circ \cong 0.08$ for those strands. In contrast, a reference experiment made for a Gel-U sample composed of monodisperse strands ($M_c = 15 \times 10^3$; including densely trapped entanglements) indicated that λ_{\max} of this gel was close to λ_{\max}° ; $\lambda_{\max} \cong 14$, $\lambda_{\max}^\circ = 16$, and $\lambda_{\max}/\lambda_{\max}^\circ \cong 0.9$ for Gel-U. These results suggested that the low- M fractions of the strands in the Gel-1/1 sample were highly stretched and broken at λ much smaller than the λ_{\max}° defined for the average M_c , thereby governing the nonlinear elongational behavior/rupture of Gel-1/1. Under large step shear strains γ (> 2), Gel-1/1 exhibited nonlinear decay of the shear stress with time. Analysis of the linear viscoelastic moduli of Gel-1/1 after imposition of large strains indicated that the stress decay under large strains reflected scission of the low- M fractions of the gel strands as well as the motion of scission-formed long strands occurring with time. This behavior was qualitatively similar to the nonlinear elongational behavior, although a delicate difference related to time-dependent cessation/motion of the scission-formed long strands remained between the nonlinearities under the large shear and elongation.

KEY WORDS: Scarcely Crosslinked Siloxane Gel / Polydisperse Gel Strands / Large Deformation / Strand Scission /

The rubber elasticity has been one of the most important subjects in the field of polymer physics, and the relationship(s) between the mechanical properties and the network structure of rubbers/gels has been studied over several decades. In the early studies, Flory¹ and James and Guth² showed that the fluctuation of the crosslinking points reduces the equilibrium modulus compared to the modulus expected for the affine displacements of these points. Langley³ and Dossin and Graessley⁴ demonstrated that the modulus is enhanced by the trapped entanglement (permanent knot) between the network strands, and Murakami *et al.*⁵ suggested a chemo-rheological method for determining the molecular weight between crosslinks. After these pioneering studies, several new aspects have been revealed for natural rubbers (crosslinked *cis*-polyisoprenes). For example, Toki *et al.*⁶ examined X-ray diffraction from natural rubbers exhibiting the elongation-induced crystallization to discuss the length distribution of the rubber strands therein.

Extensive studies were also made for model rubbers/gels prepared *via* end-crosslinking of poly(dimethyl siloxane) (PDMS) prepolymers of known molecular weights. The PDMS rubbers/gels have been chosen as the model systems because PDMS is free from the strain-induced crystallization (thereby enabling us to examine the behavior of flexible chain network under large deformation) and also because monodisperse

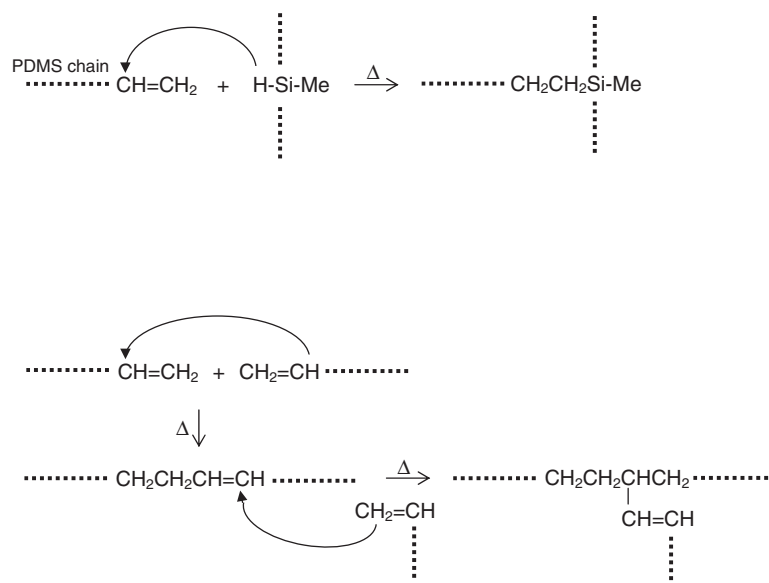
PDMS prepolymers are available in a wide range of molecular weight and these prepolymers can be chemically modified rather easily. For such PDMS rubbers/gels, the critical gelation behavior⁷ and the fractal structure on this gelation^{8,9} were investigated, and the swelling dynamics¹⁰ as well as the spatial distance between the crosslinks¹¹ were also examined. Urayama *et al.*^{12–16} made a series of studies for well-characterized PDMS rubbers/gels to investigate interesting features of these rubbers/gels such as the temperature-insensitive loss tangent. Furthermore, they made an extensive test of molecular models for rubber elasticity so far proposed to show that a version of the slip-link model (Edwards-Vilgis model¹⁷) describes most successfully the experimental data for various modes of deformation (*e.g.*, uniaxial and biaxial elongation).¹² Their work¹² demonstrated that the essential point in the molecular theory of rubber elasticity is the treatment of the trapped entanglements.

The effect of molecular weight distribution of the PDMS rubber network strands (*i.e.*, of the PDMS prepolymers) on the rubber elasticity has been also investigated extensively.^{18–24} In particular, Mark *et al.*^{19–23} and Smith *et al.*²⁴ prepared the model rubbers having a known, bimodal distribution of the strand length (through end-linking of bimodal prepolymers) to examine the relationship between this distribution and modulus/deformation of the rubbers. However, their model rubbers

¹Toray Research Center Inc., Sonoyama, Otsu 520-8567, Japan

²Institute for Chemical Research, Kyoto University, Uji 611-0011, Japan

*To whom correspondence should be addressed (Tel: +81-774-38-3135, Fax: +81-774-38-3139, E-mail: hiroshi@scl.kyoto-u.ac.jp).



were not free from the trapped entanglements and the effect of the strand length distribution on the rubber elasticity could be extracted from the experimental data only after an analysis of the effect of the trapped entanglements.

Recently, we prepared a model PDMS gel (referred to as Gel-1) through a moderate crosslinking reaction of two types of PDMS prepolymers having vinyl groups at the chain ends.^{25,26} The Gel-1 sample contained a large fraction f_{sol} of sol chains ($f_{\text{sol}} = 0.58$; mostly unreacted prepolymers), and the sol chains appeared to have suppressed formation of densely trapped entanglements during the crosslinking reaction. Thus a very scarcely crosslinked network structure was formed in Gel-1. In a linear viscoelastic test, this gel behaved as a soft elastomer and exhibited a surprisingly small mechanical loss tangent (<0.01) because of the lack of densely trapped entanglements. Analysis of the linear viscoelastic modulus suggested that the strands in Gel-1 had a very broad distribution in their molecular weight. Consequently, Gel-1 is expected to serve as a good model system for an investigation of the effect of the gel strand length distribution on the mechanical properties without being disturbed by the trapped entanglements.

Thus, we re-prepared the scarce PDMS gel (referred to as Gel-1/1) and examined its nonlinear mechanical behavior under constant-rate elongation and large step shear strains. In the elongational test, Gel-1/1 exhibited strain hardening followed by a macroscopic rupture. The elongational ratio at rupture was significantly smaller than that expected for a gel composed of monodisperse strands, suggesting that the low molecular weight (M) fraction of the gel strands was highly stretched and broken under rather small elongation thereby governing the strain-hardening/rupture of the Gel-1/1 system. In the step shear tests, Gel-1/1 showed significant stress decay with time that was also related to the scission of those low- M strands. Details of these results are reported in this paper.

EXPERIMENTAL

Materials

Commercially available two vinyl-terminated PDMS prepolymers (SE1886; Toray-Dow Corning Co., Ltd) were used. These prepolymers were from the same batches as those utilized in the previous work.^{25,26} The prepolymer-A, a neat PDMS having vinyl groups at the ends, had the weight-average molecular weight and polydispersity index of $M_w = 34.7 \times 10^3$ and $M_w/M_n = 2.6$.²⁵ The prepolymer-B, a chemically modified PDMS with a small fraction (0.7 mol %) of the dimethyl siloxane units being replaced by monomethyl siloxane units, had $M_w = 35.1 \times 10^3$ and $M_w/M_n = 3.1$.²⁵

The prepolymers A and B were mixed at a weight ratio of $w_A/w_B = 1/1$ and allowed to react at 120 °C for 3 h to give the as-prepared gel referred to as Gel-1/1. As shown in the top part of Scheme 1, the heat (at 120 °C) and a catalyst contained in the commercial prepolymers allowed the vinyl groups at the ends of prepolymers A and B to react with the monomethyl siloxane group in the prepolymer B to form the crosslinks.²⁵ In addition to this major reaction, two vinyl groups can also react with each other to give the crosslinks (bottom part of Scheme 1), though this minor reaction occurred less frequently.²⁵

The Gel-1/1 thus prepared contained a large amount of sol chains. The sol fraction f_{sol} therein was determined from a sol extraction test, as done in the previous work.²⁵ In this test, a small sheet specimen of Gel-1/1 (described later) was soaked in fresh toluene (good solvent for PDMS) for 48 h, with toluene being replaced in every 12 h. All sol chains were extracted with this procedure, and the sol fraction in the as-prepared Gel-1/1, $f_{\text{sol}} = 0.53$, was evaluated from the weights of the dry specimen before and after the sol extraction. This f_{sol} value

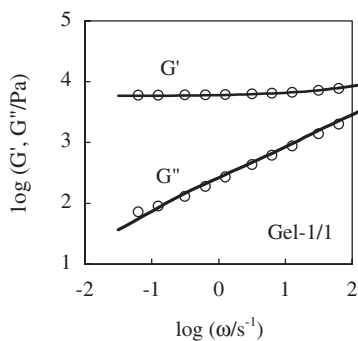


Figure 1. Linear viscoelastic moduli of as-prepared (neat) Gel-1/1 system at 20°C. The solid curves indicate the results of fitting with the Rouse network model. The strand molecular weight distribution obtained from the fitting is summarized in Table I. For further details, see text.

was a little smaller than the value ($= 0.58$) for the previously utilized Gel-1.

The sol chains extracted from the Gel-1/1 specimen were characterized with low-angle laser light scattering (LALS) and gel permeation chromatography (GPC) utilizing a LALS photometer (KMX-6, Chromatrix Co. Ltd) and a GPC unit (Model510, Waters Co. Ltd) connected to a differential refractive index detector (RI-8020, Tosoh Co. Ltd). The solvent was toluene, and commercially available monodisperse polystyrenes (TSK, Tosoh Co. Ltd) were utilized as the LALS/elution standards. The weight-average molecular weight and the polydispersity index of the sol chains, $M_{w,sol} = 45.8 \times 10^3$ (determined from LALS) and $M_{w,sol}/M_{n,sol} = 4.1$ (evaluated from GPC calibration), were not significantly different from those of the prepolymers. Thus, quite a large fraction of the prepolymers was left unreacted during the preparation of Gel-1/1.

These results indicated that the gel network in the Gel-1/1 sample was very scarce ($f_{gel} = 1 - f_{sol} = 0.47$) and not identical to a regular network formed through full end-linking of the prepolymers. This scarce network structure of Gel-1/1 (hardly having the trapped entanglement^{25,26}) was composed of highly polydisperse strands, as revealed from analysis of its linear viscoelastic moduli (*cf.* Figure 1 shown later).

The Gel-1/1 sample was subjected to constant-rate elongational tests and step shear tests. The specimens for the elongational test were prepared through the above reaction made in a small metal mold of thickness $\cong 1.0$ mm. The resulting Gel-1/1 sheet was cut with a razor into rectangular specimens of length $\cong 20$ mm and width $\cong 10$ mm to be utilized in the test. The step shear test was made in a cone-plate (CP) geometry. Since the flat sheet sample could not fit in this geometry, the specimens for the step shear test were prepared through the reaction directly made in the CP fixture mounted in a rheometer chamber. (An extra material squeezed out of the fixture was carefully removed with a razor after the reaction.)

A PDMS gel being composed of monodisperse strands was utilized as a reference material for the elongational test. This

gel, identical to the NL-138 sample in Ref. 27 and referred to as Gel-U in this study, was generously supplied from Prof. Urayama at Kyoto University. He synthesized the gel through tetrafunctional end-linking of monodisperse PDMS prepolymer ($M_n = 84 \times 10^3$) in bulk in the presence of unreactive, guest homo-PDMS chains ($M_w = 138 \times 10^3$; $f_{guest} = 15$ vol % in the system).²⁷ Gel-U had the equilibrium shear modulus of $G_e \cong 1.4 \times 10^5$ Pa at 30°C (*cf.* Figure 1 of Ref. 27). The corresponding molecular weight of the effective gel strands, $M_c = \rho(1 - f_{guest})RT/G_e \cong 15 \times 10^3$ ($\rho =$ PDMS density, $R =$ gas constant, and $T =$ absolute temperature), was considerably smaller than the prepolymer molecular weight (84×10^3) and rather close to the entanglement molecular weight ($M_e \cong 8.1 \times 10^3$ for PDMS²⁸), indicating that Gel-U prepared through the end-linking reaction in bulk contained densely trapped entanglements.²⁷ This Gel-U sample, supplied in a form of thick disk of the thickness $\cong 5$ mm, was carefully sliced with a razor into rectangular specimens of the thickness $\cong 1$ mm, length $\cong 20$ mm, and width $\cong 10$ mm, and these specimens were utilized in the elongational test.

Measurements

For the Gel-1/1 and Gel-U rectangular specimens, the true elongational stress σ_E (not the engineering stress reduced to unit cross-sectional area before the elongation) was measured under constant-rate strain at 20°C (room temperature). An extensional viscosity fixture (EVF) attached to a laboratory rheometer (ARES, Rheometrics Co. Ltd; currently TA Instruments) was utilized for the measurement, and the elongational strain rate was set at 0.01 and 0.1 s⁻¹. In EVF, the specimen was wound onto a rotating shaft to be subjected to the constant-rate elongation. Small ledges made of a silicone adhesive were attached to the pulling edges of the specimen, and the specimen was gripped at these ledges by metal pins of EVF. These ledges were helpful for start-up of winding without slippage of the specimen.

Step shear tests were conducted for Gel-1/1 at 20°C (room temperature) with a cone-plate (CP) fixture of diameter = 20 mm and gap angle = 2 deg mounted on a laboratory rheometer (Soliquid-meter, Reoraji Co. Ltd). Each specimen was subjected to a step shear strain γ in a range of $\gamma = 0.01$ –5.1, and the shear stress $\sigma(t, \gamma)$ was measured as a function of time t (up to 10000 s) after imposition of strain. The measured stress was converted to an *apparent* relaxation modulus, $G(t, \gamma) = \sigma(t, \gamma)/\gamma$. For each run of the step shear test, the specimen was freshly prepared in the CP fixture with the method explained earlier.

Before and after each run of this test, the sample prepared in the CP fixture was monitored through dynamic measurements in the linear viscoelastic regime (oscillatory strain amplitude ≤ 0.3). The storage and loss moduli, G' and G'' , measured *before* the step shear test were indistinguishable for all runs, confirming that the crosslinking reaction for the sample preparation was reproducibly achieved and the specimen was firmly gripped in the fixture in each run. The G' and G'' measured *after* the step shear test decreased with increasing

$\gamma > 2$. These moduli were utilized to characterize the network structure in the Gel-1/1 specimens that experienced the large strain.

RESULTS AND DISCUSSION

Linear Viscoelastic Behavior of As-prepared Gel-1/1

For the as-prepared Gel-1/1 sample that experienced no large strain, Figure 1 shows the angular frequency (ω) dependence of the storage and loss moduli, G' and G'' , measured at 20 °C (room temperature). G' is quite insensitive to ω , while G'' is much smaller than G' at low ω and exhibits the Rouse-like power-law behavior, $G'' \propto \omega^n$ with $n \cong 0.5$. These features are characteristic to a gel network hardly having trapped entanglements.^{25,26} A large fraction of the sol chains ($f_{\text{sol}} = 0.53$; mostly prepolymers) remained in Gel-1/1, and these sol chains possibly suppressed the trapped entanglement formation during the gelation process (crosslinking process; Scheme 1), as fully discussed in the previous studies.^{25,26}

The elasticity of the as-prepared Gel-1/1 sample is characterized with the equilibrium shear modulus G_e ($= G'(\omega \rightarrow 0)$) and the average molecular weight M_c of the gel strands: $M_c = C_{\text{gel}}RT/G_e = \rho(1 - f_{\text{sol}})RT/G_e$ where C_{gel} is the mass concentration of the gel strands in Gel-1/1, ρ is the density of Gel-1/1 as a whole, R is the gas constant, and T is the absolute temperature. From the G' data shown in Figure 1, G_e and M_c are evaluated as

$$G_e = 6.0 \times 10^3 \text{ Pa}, \quad M_c = 190 \times 10^3 \quad (1)$$

This M_c is much larger than the molecular weights of the prepolymers A and B, confirming that a scarce gel network was formed in the Gel-1/1 sample.

A comment needs to be added for the above G_e and M_c values. In the previous studies,^{25,26} the PDMS prepolymers A and B from the same batches as utilized in this study were allowed to react at the same mixing ratio as in this study ($w_A/w_B = 1/1$) to give a gel referred to as Gel-1. Nevertheless, Gel-1 had $G_e = 2.8 \times 10^3 \text{ Pa}$ and $M_c = 340 \times 10^3$ and was softer than Gel-1/1 prepared in this study. This difference could be partly due to an uncontrolled thermal history in the gel preparation process. The current Gel-1/1 specimens for the shear tests (Figure 1 and Figures 4 and 5 shown later) and elongational tests (shown later in Figure 2), respectively, were prepared in the small cone-plate (CP) fixture and the thin metal mold (of thickness $\cong 1 \text{ mm}$), as explained earlier. In both cases, the prepolymer mixture was rapidly heated to the set temperature (120 °C) to start the crosslinking reaction quickly, because the CP fixture and thin mold had small heat capacities (and the reaction in the CP fixture was made under forced convection in the rheometer chamber). In contrast, the previously utilized Gel-1 was prepared in a thicker metal mold (of thickness = 2–3 mm) having a larger thermal capacity, and the reaction started rather slowly. However, the Gel-1/1 specimens utilized in this study were reproducibly prepared in the small fixture/thin mold (as confirmed from the reproducibility of their linear viscoelastic moduli shown in

Figure 1), which enabled us to unequivocally examine the properties of the network in Gel-1/1.

Molecular Weight Distribution of As-prepared Gel-1/1 Strands

For the gel network composed of *monodisperse* strands, all strands relax at the same rates. Thus, for such gels, G'' exhibits its terminal tail ($G'' \propto \omega$) at low ω where G' becomes independent of ω .^{25,26} However, Figure 1 demonstrates that the Gel-1/1 system shows the non-terminal power-law behavior ($G'' \propto \omega^n$ with $n \cong 0.5$) at $\omega < 1 \text{ s}^{-1}$ where G' is quite insensitive to ω . This result unequivocally indicates that the gel strands therein have a broad molecular weight distribution, as fully discussed previously.^{25,26}

The width of this distribution can be estimated by fitting the G' and G'' data shown in Figure 1 with a Rouse network model:^{25,26}

$$G'(\omega) = \sum_i \left[\frac{C_i RT}{M_i} \left\{ 1 + \sum_{p \geq 1} \frac{\omega^2 (\tau_i/p^2)^2}{1 + \omega^2 (\tau_i/p^2)^2} \right\} \right] \quad (2a)$$

$$G''(\omega) = \eta_{\text{sol}} \omega + \sum_i \left[\frac{C_i RT}{M_i} \sum_{p \geq 1} \frac{\omega (\tau_i/p^2)}{1 + \omega^2 (\tau_i/p^2)^2} \right] \quad (2b)$$

Here, C_i is the mass concentration of the i -th component of the strands having the molecular weight M_i , and τ_i is the longest relaxation time of this component. The set of C_i satisfies a relationship, $\sum_i C_i = \rho(1 - f_{\text{sol}})$ with ρ being the density of the Gel-1/1 system as a whole. η_{sol} is the viscosity of the sol chains in Gel-1/1. (At the frequencies examined in Figure 1, the sol chains of $M_{w,\text{sol}} = 45.8 \times 10^3$ have fully relaxed and contributed only to G'' as a viscous component;²⁶ also see Appendix A). The relaxation time of the strands is expressed in the Rouse form,

$$\tau_i = \tau^* M_i^2 \quad (\tau^* = \text{reference time}) \quad (3)$$

Since $M_{w,\text{sol}} (= 45.8 \times 10^3)$ of the sol chains is larger than the entanglement molecular weight for PDMS, $M_e = 8.1 \times 10^3$,²⁸ η_{sol} of the sol chains is affected by the entanglement with the gel strands as well as the entanglement among the sol chains. From the bulk viscosity data of entangled linear PDMS chains, η_{sol} of those sol chains was estimated to be 3 Pa s with the method explained in Appendix A. Utilizing this η_{sol} value, we attempted to fit the G' and G'' data of Gel-1/1 with eq 2 to estimate the molecular weight distribution of the strands. In Figure 1, the solid curves indicate the best fit results obtained for the reference time $\tau^* = 8.7 \times 10^{-14} \text{ s}$ and the M_i and C_i values specified in Table I. (This set of $\{M_i, C_i\}$ is later shown in Figure 6 as the C_i vs M_i plots.) A good fit seen Figure 1 enables us to estimate the polydispersity index of the Gel-1/1 strands as

$$\frac{M_w}{M_n} = \frac{\left\{ \sum_i C_i M_i \right\} \left\{ \sum_i C_i M_i^{-1} \right\}}{\left\{ \sum_i C_i \right\}^2} \cong 600 \quad (4)$$

This result suggests that the strands in Gel-1/1 have a very broad molecular weight distribution, which corresponds to the scarce network structure having the average strand molecular weight $M_c \gg M_{\text{prepolymer}}$ (cf. eq 1).

Here, a comment needs to be made for the above fitting process where M_i was chosen rather arbitrary and C_i was determined to achieve the best fit of the G' and G'' data. This choice was not unique. Namely, equally good fitting was achieved for different sets of $\{M_i, C_i\}$ with M_i being chosen in a range similar to that of Table I. However, the polydispersity index of the gel strands was not significantly different for those sets of $\{M_i, C_i\}$, suggesting a reliability of this index given in eq 4. In this sense, the set of M_i chosen with an interval of one decade (Table I) is to be regarded as a representative, coarsened set of M_i for the actual Gel-1/1 strands. This set of M_i is later utilized in the characterization of Gel-1/1 after the imposition of large step strains.

An additional comment is to be made for the reference time τ^* appearing in eq 3. In the previous study,²⁵ the entanglement-free, intrinsic Rouse relaxation time for $M_c = 8.1 \times 10^3$ was estimated from the viscoelastic data of linear homo-PDMS as $\tau_e = 2.8 \times 10^{-7}$ s. From this τ_e value, the reference time for the intrinsic Rouse motion is obtained as $\tau_{\text{int}}^* = \tau_e/M_c^2 = 4.3 \times 10^{-15}$ s. This τ_{int}^* is considerably smaller than τ^* ($= 8.7 \times 10^{-14}$ s) giving the good fit in Figure 1. Namely, the Rouse-like relaxation seen in Figure 1 is attributable to the constraint release (CR) Rouse motion of temporarily (non-permanently) entangled gel strands. Further discussion of this CR-Rouse motion has been given elsewhere.^{25,26}

Elongational Behavior of Gel-1/1

For the as-prepared Gel-1/1 sample having significantly polydisperse strands, the true elongational stress σ_E was measured at 20 °C (room temperature) at constant Hencky strain rate, $\dot{\epsilon} = 0.01$ and 0.1 s^{-1} . In Figure 2, the σ_E data normalized by the equilibrium tensile modulus in the linear viscoelastic regime, $3G_c$ (with G_c given in eq 1), are double-logarithmically plotted against the Hencky strain ϵ ($= \ln \lambda$ with λ being the elongational ratio). The σ_E data are insensitive to the strain rate $\dot{\epsilon}$ ($\leq 0.1 \text{ s}^{-1}$). This behavior is consistent with the almost purely elastic behavior seen at angular frequencies $\omega < 1 \text{ s}^{-1}$ (cf. Figure 1). The weak relaxation process characterized by the power-law behavior of G'' ($\propto \omega^n$; $n \cong 0.5$) has a very minor contribution to the stress of the system at those low ω . Thus, the σ_E data measured at similarly low $\dot{\epsilon}$ (Figure 2) are hardly contributed from this relaxation process. These data characterize the Gel-1/1 network structure under elongation.

Table I. Molecular weight distribution of gel strands utilized for the fit in Figure 1

$10^{-3}M_i$	$C_i/\text{g cm}^{-3}$
5	0.00376
50	0.0705
500	0.0893
5000	0.108
50000	0.103
500000	0.0987

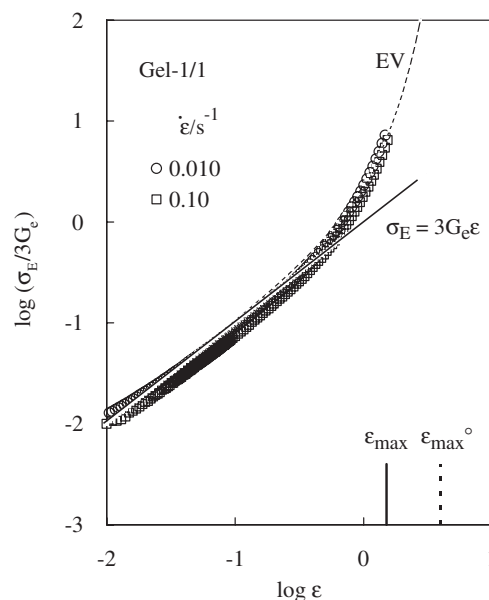


Figure 2. Elongational behavior of Gel-1/1 system at 20 °C. The solid curve indicates the elastic behavior expected from the linear viscoelastic moduli of as-prepared (neat) Gel-1/1. The dotted curve indicates the result of fitting with the Edward-Vilgis model. For further details, see text.

As seen in Figure 2, Gel-1/1 exhibits the linear elastic behavior, $\sigma_E/3G_c\epsilon = 1$ (solid line), under small elongation at $\epsilon < 0.5$ ($\lambda < 1.7$). For larger ϵ and λ , σ_E becomes larger than that expected for this linear behavior, and the macroscopic rupture occurs at $\epsilon_{\text{max}} = 1.5$ ($\lambda_{\text{max}} = 4.5$) after this hardening. This behavior is *qualitatively* similar to usual crosslinked rubbers/gels. For example, Figure 3 shows the σ_E data for the Gel-U sample having *monodisperse* strands with trapped entanglements (and containing 15 wt % of the guest sol chains of $M_n = 138 \times 10^3$) measured in this study at 20 °C. These data, normalized by the G_c data in literature ($\cong 1.4 \times 10^5 \text{ Pa}$)²⁷ and plotted against ϵ , clearly indicate the nonlinear hardening/rupture after the linear elastic behavior at small ϵ .

Thus, the strand length polydispersity in Gel-1/1 has no qualitative effect on the nonlinear elongational behavior. However, this distribution should have a *quantitative* effect. For an examination of this effect, we may compare the σ_E data with the Edward-Vilgis (EV) slip-link model.¹⁷ This molecular model, formulated for a network of *monodisperse* strands, is known to describe the rubber elasticity most accurately.¹² In this model, the elongational stress σ_E was originally expressed in terms of the elongational ratio λ , the number densities N_C and N_S of chemically crosslinked network strands and slip-links (trapped entanglements), the link-slippage parameter η , and the extensibility parameter α .¹⁷ This σ_E can be re-written as a function of λ , the number density ratio $\theta = N_S/N_C$, η , α , and the equilibrium shear modulus G_e .²⁹ The explicit form of this function is shown in Appendix B.

The parameter α is identical to the reciprocal of the maximum possible elongational ratio $\lambda_{\text{max}}^\circ$ defined for the sub-strand between trapped entanglement points (in the presence of

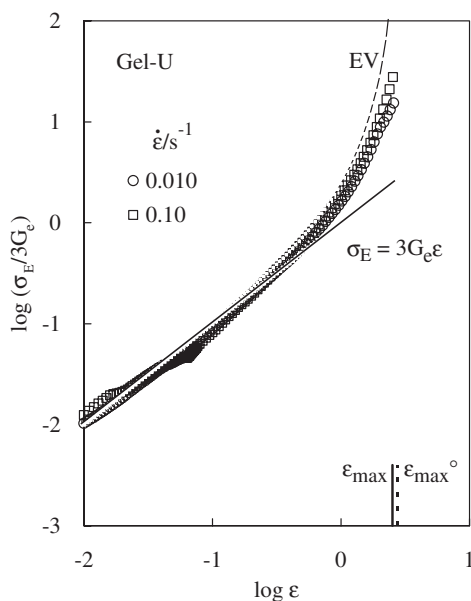


Figure 3. Elongational behavior of Gel-U system at 20°C. The solid curve indicates the elastic behavior expected from the linear viscoelastic moduli of Gel-U, and the dotted curve indicates the result of fitting with the Edward-Vilgis model. For further details, see text.

these entanglements) and for the strand as a whole (in the absence of the entanglements). The Gel-1/1 system hardly includes the trapped entanglements while the Gel-U system has densely trapped entanglements, as explained earlier. For both systems, α can be given by $1/\lambda_{\max}^\circ$, with λ_{\max}° being evaluated from the strand molecular weight M_c evaluated from G_c . (For Gel-U, M_c is the molecular weight of the trapped entanglement strands, not the neat strands equivalent to the PDMS prepolymer.) The λ_{\max}° values thus calculated are:

$$\lambda_{\max}^\circ \equiv \frac{\langle R_c^2 \rangle^{1/2}}{b_K} = 53 \text{ (for Gel-1/1), } 16 \text{ (for Gel-U)} \quad (5)$$

Here, $\langle R_c^2 \rangle$ is the mean-square end-to-end distance of the strand of the molecular weight M_c under no external elongation ($\langle R_c^2 \rangle = 0.00422M_c \text{ nm}^2$ for PDMS³⁰), and b_K is the Kuhn step length (= 0.53 nm for PDMS³¹): b_K is identical to a ratio of $\langle R_c^2 \rangle$ to the full-stretch length of the strand.

A comment needs to be made for the λ_{\max}° value for the Gel-1/1 system. The M_c value of this system (= 190×10^3 ; eq 1) is an average over the polydisperse strands therein and thus the λ_{\max}° obtained from M_c is also regarded as an average. Despite this polydispersity, the use of the average λ_{\max}° seems to allow the application of the EV model (formulated for monodisperse strands) to the Gel-1/1 system with the highest consistency.

Utilizing the G_c data and the above λ_{\max}° values (= $1/\alpha$) in the EV model summarized in Appendix B, we calculated σ_E of the Gel-1/1 and Gel-U systems as a function of ε (= $\ln \lambda$). The results are shown in Figures 2 and 3 with the dashed curves. The vertical dotted lines indicate $\varepsilon_{\max}^\circ = \ln \lambda_{\max}^\circ$. For definiteness, we set $\eta = 0$ and utilized θ as a fitting parameters to achieve the best fit of the data. The calculated σ_E was

insensitive to the θ value given that θ was set below 0.2 (20% population of the slip-links compared to the chemical cross-links). Thus, our treatment of the parameters θ and η introduced little uncertainty in the model fitting. In Figures 2 and 3, the curves calculated for $\eta = 0$ and $\theta = 0.05$ are shown.

As seen in Figures 2 and 3, the σ_E data of the Gel-1/1 and Gel-U systems are close to the EV calculation made for monodisperse strands. In this sense, the strand length polydispersity in the Gel-1/1 system appears to have little effect on the elongational behavior. However, a remarkable effect is noted for the maximum strain at rupture, ε_{\max} , shown with the vertical solid lines. For the Gel-U system prepared by end-linking of monodisperse prepolymer chains (*neat strands*), ε_{\max} is close to ε_{\max}° defined for the trapped entanglement strands therein; $\varepsilon_{\max} \cong 0.9\varepsilon_{\max}^\circ$ and $\lambda_{\max} \cong 0.8\lambda_{\max}^\circ$ for Gel-U. This result indicates that most of the trapped entanglement strands therein are stretched but not broken until the macroscopic rupture occurs. (In fact, the rupture point is not very far even from the full-stretch point ($\lambda_{\max, \text{neat}}^\circ \cong 36$) defined for the longer, neat strands with $M_n = 84 \times 10^3$; $\lambda_{\max} \cong 0.4\lambda_{\max, \text{neat}}^\circ$.)

In contrast, for the Gel-1/1 system, ε_{\max} is considerably smaller than ε_{\max}° , giving $\lambda_{\max} \cong 0.08\lambda_{\max}^\circ$. This result suggests that low- M fractions of the polydisperse strands are highly stretched and broken at rather small $\lambda \ll \lambda_{\max}$ because λ_{\max}° decreases with decreasing M ; $\lambda_{\max}^\circ \propto M^{1/2}$ as seen from eq 5. Thus, the hardening/rupture of Gel-1/1 appears to be governed by the short strands, demonstrating the important effect of the strand length polydispersity on the toughness of the gel: The toughness is reduced as the strands become polydisperse. This effect is further discussed below in relation to the stress decay of Gel-1/1 under large step strains.

Stress Decay of Gel-1/1 under Large Step Shear

The Gel-1/1 specimens were subjected to step shear strains of various magnitudes γ (≤ 5.1) at 20°C (room temperature), and the shear stress $\sigma(t, \gamma)$ was measured with time t up to 10000 s. Figure 4 shows changes of the apparent relaxation modulus $G(t, \gamma)$ ($= \sigma(t, \gamma)/\gamma$) with t . For $\gamma \leq 2$, $G(t, \gamma)$ remains independent of t and its value agrees with the equilibrium modulus in the linear viscoelastic regime, $G_e = 6.0 \times 10^3$ Pa (eq 1). Thus, no shear-induced change (scission) occurred for the Gel-1/1 network at $t \leq 10000$ s and $\gamma \leq 2$. In contrast, for larger $\gamma \geq 2.6$, $G(t, \gamma)$ decays with t significantly, and the decay is faster and larger for larger γ . This nonlinear decay should be contributed not only from a molecular relaxation process (gel strand motion) but also from the strand scission, as discussed later for Figures 5 and 8. In this sense, $G(t, \gamma)$ of Gel-1/1 shown here is qualitatively different from the nonlinear relaxation modulus of uncrosslinked homopolymer chains that detects only the non-equilibrium chain motion.³² (For this reason, we referred to $G(t, \gamma)$ of Gel-1/1 as the *apparent* relaxation modulus.)

Figure 5 shows the linear viscoelastic moduli of the Gel-1/1 specimens measured after the imposition of step strains γ for 10000 s. For clarity of Figure, only the data for representative γ values are shown. The moduli after the imposition of strain

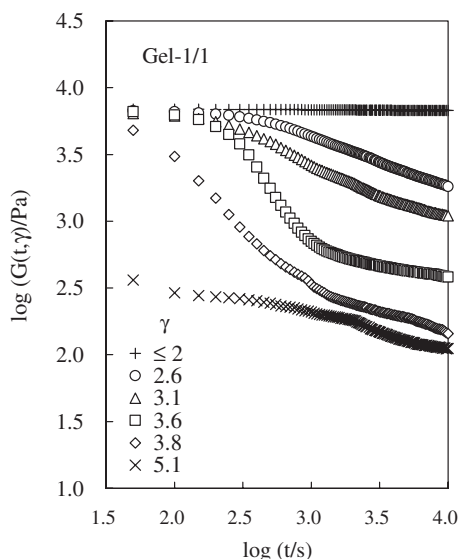


Figure 4. Nonlinear stress decay behavior of Gel-1/1 system subjected to step shear strains of various magnitudes γ .

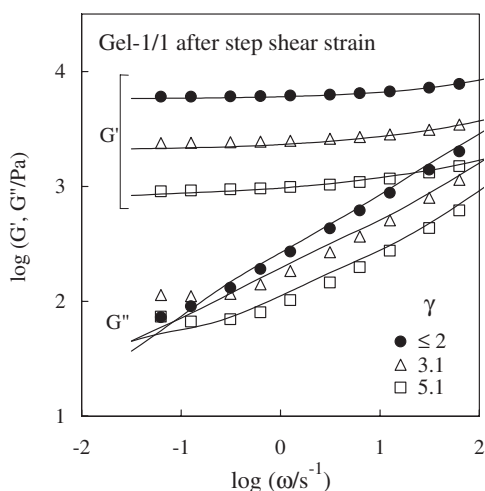


Figure 5. Linear viscoelastic moduli of Gel-1/1 system measured after imposition of step shear strains of various magnitudes γ . The solid curves indicate the results of fitting with the Rouse network model. The strand molecular weight distributions obtained from the fitting are shown in Figure 6.

$\gamma \leq 2$ were indistinguishable from those before the imposition, confirming that the gel network was not broken at those γ . For larger γ , the storage modulus G' still exhibits a low- ω plateau but this plateau height decreases with increasing γ . This decrease unequivocally indicates that the gel network sustaining the G' plateau was partly broken by the large step strains to decrease the number density of the elastically effective strands. (The network was not fully broken in the range of γ examined, as noted from the long-time plateau of $G(t, \gamma)$ and low- ω plateau of G' .)

Some details of this partially broken network structure can be examined for the loss modulus, G'' . As noted in Figure 5, G'' at high ω decreases significantly while G'' at low ω hardly decreases (or even slightly increases) after the imposition of

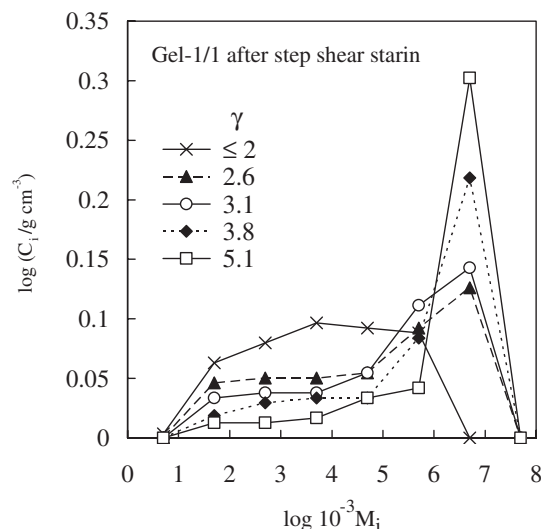


Figure 6. The strand molecular weight distribution of Gel-1/1 after imposition of shear strain. The distribution was obtained from the fitting with the Rouse network model (cf. Figure 5).

large step strains. Thus, the disruption of the gel network is expected to have occurred from the short strands (governing the high- ω response of the system) to long strands on the increase of γ . We can test this expectation by fitting the G' and G'' data with the Rouse network model (eq 2). In eq 2, we utilized the strand molecular weights M_i (Table I) and the strand relaxation times τ_i (eq 3) identical to those for the as-prepared Gel-1/1 specimen (Figure 1) and attempted to estimate the mass concentrations of the strands C_i from the fit of the data after the large step shear. The solid curves in Figure 5 shows the best-fit results, and Figure 6 shows the corresponding set of C_i plotted against M_i . (The plot for $\gamma \leq 2$ represents the $\{M_i, C_i\}$ set summarized in Table I.) Figure 6 demonstrates that the concentration decreases and increases, respectively, for the low- M and high- M strands with increasing γ . The set of M_i utilized here is to be regarded as a representative, coarsened set of M_i for the actual Gel-1/1 strands, as explained earlier. However, the result seen in Figure 6 qualitatively confirms the above expectation without ambiguity.

Here, a comment needs to be made for the increase of the long strand concentration with increasing γ . One may suspect that the shear-induced disruption of the network just results in the decrease of the short strand concentration and does not enrich the long strands. If the short and long strands fully segregate in space, this type of network disruption could certainly occur. However, if the short and long strands are mixed in space (which seems to be the case for the Gel-1/1 system), some short strands bridge the long strands as shown schematically in the top part of Figure 7; see, for example, two short strands marked with asterisk. Then, the scission of such short strands converts these strands into short dangling chains and, at the same time, releases the bridging point between the long strands to convert these long strands into longer strands carrying the short dangling chains; see the middle part of

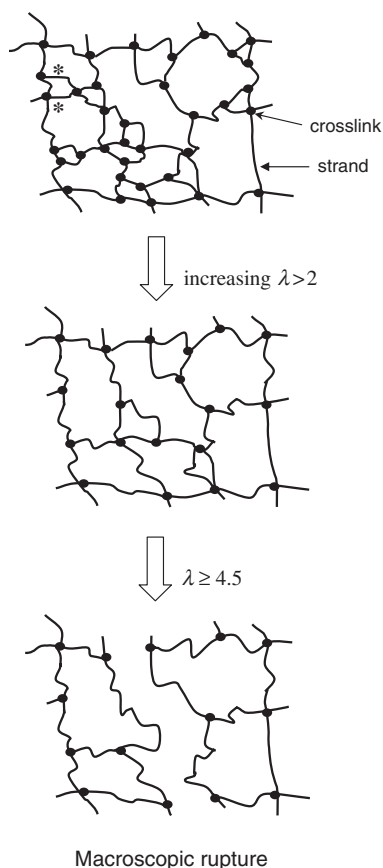


Figure 7. Schematic illustration of the mode of scission of the gel network in Gel-1/1.

Figure 7 (where the dangling chains are not shown for simplicity). In other words, the scission of the short strands tends to enrich the longer strands. The increase of the long strand concentration seen in Figure 6 appears to reflect this mode of network disruption.

We note an interesting consequence of this network disruption mode. If the scission of the short strands enriches the long strands that are even longer than the strands existing in the as-prepared Gel-1/1, the elongational rupture strain ε_{\max} of Gel-1/1 may increase when the system is subjected to a moderately large shear in prior to the elongation. A test of this possibility is an interesting subject of future work.

Comparison of Gel-1/1 Network Disruption under Elongation and Shear

The nonlinear elongational and shear behavior of Gel-1/1 seen in Figures 2 and 4 commonly reflects the scission of the gel strands (that starts from short strands and propagates to long strands), as discussed earlier. This similarity of the elongational and shear behavior can be further examined for the elongational ratio λ_s under the step shear strain of the magnitude γ ; $\lambda_s = (1 + \gamma^2/3)^{1/2}$ for the affine deformation. For the maximum shear strain examined, $\gamma = 5.1$, the modulus $G(t, \gamma)$ at long times decayed by a factor of ~ 50 compared to $G(t, \gamma)$ before the shear imposition (*cf.* Figure 4) and the

Gel-1/1 sample was *almost* macroscopically disrupted. The corresponding λ_s value ($= 3.1$) is fairly close to the λ_{\max} value ($= 4.5$) at the elongational rupture point, demonstrating the similarity of the elongational and shear nonlinearities of Gel-1/1. However, we also note a delicate difference between these nonlinearities, as discussed below.

As explained for Figure 7, the scission of short strands yields a long strand. This long strand would have a distorted conformation when it is formed, and its motion can result in relaxational decay of the stress. If this long strand has the maximum elongational ratio λ_{\max}° (defined by eq 5) comparable to/smaller than λ_s , its scission should also contribute to the stress decay. The very gradual decay of $G(t, \gamma)$ under the large step shear, occurring in a range of $t \geq 1000$ s (Figure 4), would have reflected both of the motion and scission of the scission-formed long strands.

In relation to this point, it is informative to compare the storage modulus measured after imposition of the step shear, $G'(\omega = 0.06 \text{ s}^{-1})$ with 0.06 s^{-1} being the lowest ω examined in Figure 5, and the apparent relaxation modulus under step shear, $G(t = 10000 \text{ s})$ with 10000 s being the longest t examined in Figure 4. $G'(\omega = 0.06 \text{ s}^{-1})$ and $G(t = 10000 \text{ s})$ commonly exhibit the nonlinear decrease from the equilibrium modulus G_e of the as-prepared Gel-1/1 on the increase of $\gamma (> 2)$, as shown in Figure 8. More importantly, $G(t = 10000 \text{ s})$ is smaller than $G'(\omega = 0.06 \text{ s}^{-1})$ in this nonlinear regime possibly because the slow motion of the scission-formed long strands leads to the relaxation at long $t (= 10000 \text{ s})$ while this motion does not contribute the behavior at short $t (= 1/\omega = 17 \text{ s})$ corresponding to $\omega = 0.06 \text{ s}^{-1}$.

In relation to this time scale of the motion/relaxation of the scission-formed long strands, we note that the macroscopic rupture of the Gel-1/1 in our elongational condition occurred in the time scale of $t = \varepsilon_{\max}/\dot{\varepsilon} \leq 150 \text{ s}$ ($\varepsilon_{\max} = 1.5$ and $\dot{\varepsilon} = 0.1$ and 0.01 s^{-1} ; *cf.* Figure 2). Thus, the motion/relaxation of the scission-formed long strands should have hardly occurred in our elongational test, as similar to the situation for the G' data measured after the step shear. In this sense, the disruption behavior of Gel-1/1 under the elongation and shear (Figures 2

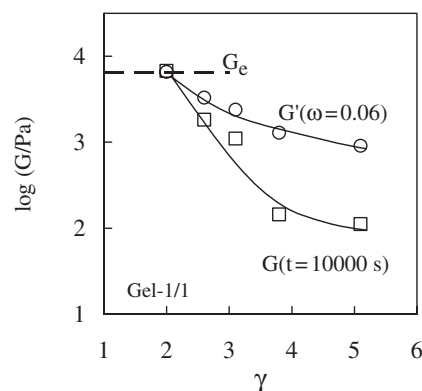


Figure 8. Comparison of the apparent relaxation modulus at long times measured under step shear strains, $G(t = 10000 \text{ s})$, and the linear storage modulus at low frequency measured after imposition of step shear strains, $G'(\omega = 0.06 \text{ s}^{-1})$.

and 4) are not identical. Nevertheless, the fundamental feature of this disruption, the scission propagating from short to long strands, is common for the elongational and shear behavior of Gel-1/1 having highly polydisperse strands.

CONCLUDING REMARKS

Nonlinear mechanical behavior was examined for a scarcely crosslinked poly(dimethyl siloxane) gel, referred to as Gel-1/1, under constant-rate elongation and large step shear. The gel strands in Gel-1/1 had an average molecular weight of $M_c = 190 \times 10^3$ and a very broad molecular weight distribution ($M_w/M_n \cong 600$), as noted from the fit of its linear viscoelastic moduli with the Rouse network model.

In the elongational test, Gel-1/1 sample exhibited the strain hardening followed by the macroscopic rupture at the elongational ratio of $\lambda_{\max} = 4.5$. This λ_{\max} was significantly smaller than the maximum elongational ratio (full-stretch ratio; $\lambda_{\max}^\circ = 53$) nominally expected for a gel composed of monodisperse strands of $M_c = 190 \times 10^3$. This difference between λ_{\max} and λ_{\max}° is attributable to the polydispersity of the strand length. Namely, the scission of the low- M fractions of the strands in Gel-1/1 should have occurred at λ much smaller than λ_{\max}° , thereby governing the nonlinear elongational behavior/rupture of Gel-1/1. The scission would have propagated from short to long strands to result in the rupture.

Under large step shear strains $\gamma (> 2)$, Gel-1/1 exhibited nonlinear decay of the shear stress with time. Analysis of the linear viscoelastic moduli of Gel-1/1 after the imposition of large strains indicated that the stress decay reflected scission of the low- M fractions of the gel strands (as well as the motion of scission-formed long strands) occurring with time. This behavior was similar to the nonlinear elongational behavior, although a delicate difference related to a time-dependent cessation/motion of the scission-formed long strands remained between the nonlinearities under the large step shear and elongation.

Acknowledgment. We thank Professor Kenji Urayama at Department of Material Chemistry, Graduate School of Engineering, Kyoto University, for helpful discussion and generous supply of his material (Gel-U).

Appendix A: Viscosity of Sol Chains in Gel-1/1

The zero-shear viscosity data for entangled bulk PDMS chains have been reported in literature.³³ As shown in our previous work,²⁵ these data are well described by an empirical equation,

$$\eta_0 = 5.0 \times 10^{-17} M_w^{3.6} \text{ (in Pa s) for bulk PDMS at } 20^\circ\text{C} \quad (\text{A}\cdot 1)$$

For the sol chains in Gel-1/1 ($M_{w,\text{sol}} = 45.8 \times 10^3$), the zero shear viscosity in the *bulk state* is estimated from eq A-1 as $\eta_0^{[\text{bl}]} = 3.0 \text{ Pa s}$ at 20°C . In the Gel-1/1 system, the sol chains should have fully relaxed at the angular frequencies ω examined in Figure 1 ($\omega \leq 10^2 \text{ s}^{-1}$), as judged from the relaxation time of bulk PDMS chains ($\tau_w/s = 1.0 \times 10^{-21} M_w^{3.6}$ at 20°C).²⁵ Thus, the sol chains in Gel-1/1 should have only a viscous contribution to G'' of the system. The viscosity corresponding to this contribution is estimated to be $f_{\text{sol}} \eta_0^{[\text{bl}]} = 1.6 \text{ Pa s}$ ($f_{\text{sol}} = 0.53$; sol fraction in Gel-1/1) if the sol chain motion is not affected by the gel strands. However, in general, the chain motion is retarded by a factor of $\cong 2$ and the viscosity is enhanced by the same factor in the presence of almost equal amount of slowly moving chains³² (= gel strands in our case). With this enhancement (due to the sol-strand entanglement), the sol viscosity in Gel-1/1 is estimated to be $\eta_{\text{sol}} \cong 2f_{\text{sol}} \eta_0^{[\text{bl}]} \cong 3 \text{ Pa s}$. This η_{sol} was utilized in the fit of the G' and G'' data of Gel-1/1 with the Rouse network model (eq 2).

Appendix B: Edwards-Vilgis Model

For rubbers containing no dangling loop/tail, Edwards and Vilgis¹⁷ derived a theoretical relationship between the uniaxial tensile force f_E and the elongational ratio λ being expressed in terms of the link-slippage parameter η and the extensibility parameter α as well as the number densities of the network strands and trapped entanglements, N_C and N_S . This f_E - λ relationship can be rearranged into a relationship between the extensional stress σ_E and λ that includes the equilibrium shear modulus G_e as a parameter. The results are summarized as²⁹

$$\frac{\sigma_E}{G_e} = \frac{f_c(\lambda; \alpha)}{g_c(\alpha) + \theta g_s(\alpha, \eta)} + \frac{f_{s1}(\lambda; \alpha, \eta) + f_{s2}(\lambda; \alpha) + f_{s3}(\lambda; \alpha, \eta) + f_{s4}(\lambda; \eta)}{\theta^{-1} g_c(\alpha) + g_s(\alpha, \eta)} \quad (\text{B}\cdot 1)$$

with

$$G_e = N_C k_B T \{g_c(\alpha) + \theta g_s(\alpha, \eta)\}, \quad \theta = N_S/N_C \quad (\text{B}\cdot 2)$$

The functions g 's and f 's appearing in eqs B-1 and B-2 are defined below.

$$g_c(\alpha) = \frac{1 - 2\alpha^2 + 3\alpha^4}{(1 - 3\alpha^2)^2}, \quad g_s(\alpha, \eta) = \frac{1 - (2 - 2\eta - 2\eta^2)\alpha^2 + (3 + 6\eta)\alpha^4}{(1 - 3\alpha^2)^2(1 + \eta)^2} \quad (\text{B}\cdot 3)$$

$$f_c(\lambda; \alpha) = \frac{\{1 - 2\alpha^2 + \alpha^4(\lambda^2 + 2\lambda^{-1})\}}{\{1 - \alpha^2(\lambda^2 + 2\lambda^{-1})\}^2} (\lambda^2 - \lambda^{-1}) \quad (\text{B}\cdot 4)$$

$$f_{s1}(\lambda; \alpha, \eta) = \frac{(1 - \alpha^2)\alpha^2(1 + \eta)}{\{1 - \alpha^2(\lambda^2 + 2\lambda^{-1})\}^2} \left(\frac{\lambda^2}{1 + \eta\lambda^2} + \frac{2}{\eta + \lambda} \right) (\lambda^2 - \lambda^{-1}) \quad (\text{B}\cdot 5)$$

$$f_{s2}(\lambda; \alpha) = \frac{-\alpha^2}{\{1 - \alpha^2(\lambda^2 + 2\lambda^{-1})\}} (\lambda^2 - \lambda^{-1}) \quad (\text{B-6})$$

$$f_{s3}(\lambda; \alpha, \eta) = \frac{(1 - \alpha^2)(1 + \eta)}{\{1 - \alpha^2(\lambda^2 + 2\lambda^{-1})\}} \left\{ \frac{\lambda^2}{(1 + \eta\lambda^2)^2} - \frac{\lambda}{(\eta + \lambda)^2} \right\} \quad (\text{B-7})$$

$$f_{s4}(\lambda; \eta) = \eta \left\{ \frac{\lambda^2}{1 + \eta\lambda^2} - \frac{1}{\eta + \lambda} \right\} \quad (\text{B-8})$$

For fitting the σ_E data of Gel-1/1 and Gel-U systems, the measured G_e data and maximum stretch ratio of the gel strands λ_{\max}° ($= 1/\alpha$) were utilized in eqs B-1 and B-2. For definiteness, we set $\eta = 0$ and utilized θ as a fitting parameters to achieve the best fit of the data. For further details, see the main text.

Received: November 20, 2007

Accepted: February 9, 2008

Published: March 26, 2008

REFERENCES

1. P. J. Flory, "Principles of Polymer Chemistry," Cornell University Press, Ithaca, New York, 1953.
2. H. M. James and E. J. Guth, *J. Chem. Phys.*, **15**, 669 (1947).
3. N. R. Langley, *Macromolecules*, **1**, 348 (1968).
4. L. M. Dossin and W. W. Graessley, *Macromolecules*, **12**, 123 (1979).
5. K. Murakami, H. Oikawa, and K. D. Suh, *Nihon Reoroji Gakkaishi*, **17**, 13 (1989).
6. S. Toki, I. Sics, S. Ran, L. Liu, and B. S. Hsiao, *Polymer*, **44**, 6003 (2003).
7. F. Chambon and H. H. Winter, *J. Rheol.*, **31**, 683 (1987).
8. T. Tixier, Ph. Tordjeman, G. Cohen-Solal, and P. H. Mutin, *J. Rheol.*, **48**, 39 (2004).
9. D. Adolf and J. E. Martin, *Macromolecules*, **24**, 6721 (1991).
10. H. Oikawa and K. Murakami, *Macromolecules*, **24**, 1117 (1991).
11. F. Horkay, A. M. Hecht, M. Zrínyi, and E. Geisslar, *Polym. Gels Networks*, **4**, 451 (1996).
12. K. Urayama, T. Kawamura, and S. Kohjiya, *Macromolecules*, **34**, 8261 (2001).
13. K. Urayama, *Nihon Reoroji Gakkaishi*, **33**, 257 (2005).
14. K. Urayama, T. Kawamura, Y. Hirata, and S. Kohjiya, *Polymer*, **39**, 3827 (1998).
15. T. Kawamura, K. Urayama, and S. Kohjiya, *Macromolecules*, **34**, 8252 (2001).
16. K. Urayama, T. Miki, T. Takigawa, and S. Kohjiya, *Chem. Mater.*, **16**, 173 (2004).
17. S. F. Edwards and T. A. Vilgis, *Polymer*, **27**, 483 (1986).
18. K. H. Schimmel and G. Heinrich, *Colloid Polym. Sci.*, **269**, 1003 (1991).
19. J. E. Mark, *Adv. Polym. Sci.*, **44**, 1 (1982).
20. M. A. Llorente, A. L. Andraday, and J. E. Mark, *J. Polym. Sci., Polym. Phys. Ed.*, **19**, 621 (1981).
21. J. E. Mark, *Acc. Chem. Res.*, **27**, 271 (1994).
22. J. E. Mark, *Rubber Chem. Technol.*, **72**, 465 (1999).
23. J. E. Mark, *Macromol. Symp.*, **201**, 77 (2003).
24. T. L. Smith, B. Haidar, and J. L. Hedrick, *Rubber Chem. Technol.*, **63**, 256 (1990).
25. H. Takahashi, Y. Ishimuro, and H. Watanabe, *Nihon Reoroji Gakkaishi*, **34**, 135 (2006).
26. H. Takahashi, Y. Ishimuro, and H. Watanabe, *Nihon Reoroji Gakkaishi*, **35**, 191 (2007).
27. K. Urayama, K. Yokoyama, and S. Kohjiya, *Macromolecules*, **34**, 4513 (2001).
28. W. W. Graessley, *Adv. Polym. Sci.*, **16**, 1 (1974).
29. H. Watanabe, Y. Matsumiya, T. Sawada, and T. Iwamoto, *Macromolecules*, **40**, 6885 (2007).
30. L. J. Fetters, D. J. Lohse, and R. H. Colby, in "Physical Properties of Polymers Handbook" 2 ed., J. E. Mark, Ed., Springer, New York, 2007, p445.
31. G. Evmenenko, H. Mo, S. Kewalramani, and P. Dutta, *Polymer*, **47**, 878 (2006).
32. H. Watanabe, *Prog. Polym. Sci.*, **24**, 1253 (1999).
33. J. A. Ressia, M. A. Villar, and E. M. Vallés, *Polymers*, **41**, 6885 (2000).